Published in final edited form as:
Biochem Biophys Res Commun. 2007 February 2; 353(1): 1–5.

Crystal Structure of the Nod1 Caspase Activation and Recruitment Domain

Nathan P. Coussens[1], **Jonathan C. Mowers**[1], **Christine McDonald**[2], **Gabriel Nuñez**[3], and **S. Ramaswamy**[1,*]

1 *Department of Biochemistry, Roy J. and Lucille A. Carver College of Medicine, the University of Iowa, Iowa City, Iowa*

2 *Department of Pathobiology, Lerner Research Institute, Cleveland Clinic Foundation, Cleveland, Ohio*

3 *Department of Pathology and Comprehensive Cancer Center, the University of Michigan Medical School, Ann Arbor, Michigan*

Abstract

Nod-like receptors (NLRs), Nod1 and Nod2 are cytosolic detectors of pathogen associated molecular patterns (PAMPs). Nod1 is a three-domain protein, consisting of a caspase activation and recruitment domain (CARD), a nucleotide-binding oligomerization domain (NOD), and a leucine-rich repeat domain (LRR). The binding of PAMPs to the LRR results in the activation of signaling through homophilic CARD-CARD interactions. Several CARD structures have been determined, including a recent NMR structure of Nod1 CARD. In contrast to the reported NMR structure, the crystal structure reported here is a dimer, where the sixth helix is swapped between two monomers. While the overall structure is very similar to the known CARD structures, this is the first report of a homodimeric CARD structure. The ability of the CARD to exist in monomeric and dimeric forms suggests another level of regulation in the activation of NLR proteins.

Keywords

Nod1; CARD4; CARD; inflammation; apoptosis; Nod Like Receptor

Introduction

Innate immunity is essential for the long-term survival of all multicellular organisms. It has evolved to provide a maximal, non-specific host response following pathogen detection. In vertebrates, it also plays a crucial role in the regulation of the adaptive immune response against invading pathogens. The system relies on a limited number of nuclear encoded pattern recognition receptors (PRRs), which are specific for pathogen associated molecular patterns (PAMPs) that are highly conserved across microbes of the same class [1]. Both cell-surface and cytosolic innate immune receptors have been identified. The human Toll-like receptors are transmembrane proteins localized to both the cell surface and lysosome/endosome compartment [2]. Recently, the proteins Nod1 and Nod2 have been identified as receptors required for the detection of enteroinvasive bacteria in the cytoplasm [3].

* Corresponding author, Fax: +1 319 335 9570, E-mail address: s-ramaswamy@uiowa.edu.

Nod1 and Nod2 belong to a larger NOD-like receptor (NLR) family of proteins with over 20 homologues in humans [3]. The NLR proteins contain three types of domains. The N-terminal domain is a variable effector-binding domain, which is involved in downstream signaling following activation. This domain can be of a variety of different types: a caspase activation and recruitment domain (CARD), a pyrin domain, a baculoviral inhibitor of apoptosis (IAP) repeat domain or a Toll/IL-1 receptor (TIR) domain. Two conserved domains include a centrally-located nucleotide-binding oligomerization domain (NOD), which acts as a nucleotide-dependent oligomerization region, and a C-terminal leucine-rich repeat (LRR), which is required for ligand recognition [3].

The Nod1 receptor is a soluble, intracellular protein that is expressed in nearly all adult tissues [4,5]. Nod1 is activated by di- or tripeptide structures with *meso*-diaminopimelic acid as the terminal amino acid [6,7]. This unusual amino acid is present in the peptidoglycan from all Gram-negative and a few Gram-positive bacteria, such as *Bacillus subtilis* and *Listeria monocytogenes*. Following ligand recognition, Nod1 activates NF-κB through a CARD-CARD interaction with RICK (receptor interacting serine/threonine kinase) [4,5,8]. Ligand-activated Nod1 has also been shown to enhance the processing of procaspase-9 to produce active caspase-9, resulting in cellular apoptosis [4]. In addition, Nod1 was shown to interact with procaspase-1, enhancing the caspase-1-induced secretion of the pro-inflammatory cytokine, interleukin-1 beta [9]. Mutations affecting the CARD of Nod1 prevented the activation of RICK [4], procaspase-9 [4], and procaspase-1 [9]. Therefore, the Nod1 CARD is thought to be essential for the downstream activation of inflammatory and apoptotic pathways.

The family of CARDs belongs to the death domain superfamily, which includes the death domain (DD) and death effector domain (DED) families [10]. The domains are all characterized by a Greek key motif of six alpha helicies. Several structures have been determined for isolated CARDs: RAIDD [11], ICEBERG [12], and Nod1 [13] by NMR and APAF-1 by X-ray crystallography [14,15] and NMR [16,17]. A crystal structure was also determined for the heterodimeric complex of APAF-1 and procaspase-9 CARDs [15]. The CARD structures determined so far are very similar. However, a primary sequence alignment reveals very low identity (< 20%). So far, structural studies have only investigated CARDs involved in apoptotic pathways. Nod1 CARD is the first pro-inflammatory CARD to be studied in atomic detail.

We report here the crystal structure of the human Nod1 CARD. A comparison of this structure with the structures of other known CARDs and with the NMR structure of Nod1 CARD [13] reveals differences that are possibly important for its function.

Materials and methods

Expression and purification of Nod1 CARD

The CARD of human Nod1, from residues serine 16 to glycine 108, was amplified by the polymerase chain reaction (PCR) using the following oligonucleotide primers: 5′- GCG CCT TCC ATA TGT CTC ACC CCC ACA TT -3′ and 5′- GAT TAT CGC TCG AGG CCG ATC TCC AGC -3′. The resulting PCR product was digested with restriction enzymes *Nde I* and *Xho I* for ligation into a pET-21a vector (Novagen). The cloning was designed to include a C-terminal poly-histidine (6-His) tag, however, amino acids leucine and glutamic acid were inserted between glycine 108 and the poly-histidine tag, due to the *Xho I* restriction site. The resulting plasmid was used to transform the *Escherichia coli* strain BL21(DE3) (Invitrogen). Transformed cells were grown at 37°C in LB medium, supplemented with ampicillin (100 μg/mL). At mid-log phase (OD_{600} ~ 0.5), overexpression of Nod1 CARD was induced with 1 mM isopropyl-D-thiogalactoside (Research Products International Corp.). The culture was harvested 4 hours after induction by centrifugation for 30 minutes at 7,280 x g and 4°C. The cells were resuspended in 45 mL of buffer A (50 mM sodium phosphate, 150 mM NaCl, 5 mM

imidazole, pH 7.0) per 1 liter of culture, and lysed using a French press at 16,000 psi. The lysate was spun for 45 minutes at 186,010 x g and 4°C to separate the soluble and insoluble fractions. The resulting supernatant was separated from the pellet and mixed with TALON metal affinity resin (BD Biosciences) pre-equilibrated in buffer A. The mixture was allowed to incubate on a rotating platform at 4°C for 5 hours, followed by centrifugation at 700 x g and 4°C for 5 minutes to pellet the resin. The supernatant was removed and the resin was washed 4 times with 30 batch volumes of buffer A. Afterwards, the resin was washed once with 30 batch volumes of high-salt buffer A (50 mM sodium phosphate, 1 M NaCl, 5 mM imidazole, pH 7.0) before elution buffer (50 mM sodium phosphate, 150 mM NaCl, 500 mM imidazole, pH 7.0) was used to elute the Nod1 CARD protein. The eluted protein was dialyzed against buffer B (20 mM Tris, 10 mM NaCl, 5 mM DTT, pH 8.0) and loaded onto a DEAE Sepharose Fast Flow column (XK 16, Amersham Biosciences) equilibrated with buffer B. After the protein was loaded, the column was washed with 55 mL of buffer B. To elute the protein, a linear gradient of buffer B containing 10 to 500 mM NaCl, with a total volume of 130 mL, was used. The flow rate was 0.5 mL/min. Nod1 CARD eluted between 200 and 250 mM NaCl. The Nod1 CARD fractions were pooled and further purified to homogeneity using gel-filtration chromatography. Gel-filtration was performed with a Superdex G-75 column (Amersham Pharmacia) equilibrated in buffer B. A total volume of 133 mL was used and the flow rate was 0.5 mL/min. The Nod1 CARD eluted as a peak centered at 80 mL. The peak fractions were pooled and concentrated to 20 mg/mL (estimated by A_{280} using an extinction coefficient of 10,095 M^{-1} cm^{-1}).

Crystallization of Nod1 CARD

The initial crystallization conditions for Nod1 CARD were obtained from the Wizard I screen (Emerald BioSystems), using the hanging-drop, vapor-diffusion method. Diffraction quality crystals were grown from drops consisting of a mixture of equal volumes of protein (20 mg/mL) and reservoir solution, containing 100 mM acetate buffer, pH 4.7, and 12–20% (w/v) PEG 3000, after 16 hours at 4°C.

Data collection and structure determination

Nod1 CARD crystals were flash frozen in mother liquor containing 10% (v/v) glycerol. The crystals were mounted in loops and used for data collection at 100 K from the GM/CA CAT beamline at the Advanced Photon Source (APS), Argonne, IL, USA. The data was collected on a MAR-CCD detector with a crystal to detector distance of 250 mm. The crystals belong to the tetragonal system. The data was processed and scaled using D*trek [18]. Systematic absences revealed that the space group was either $P4_12_12$ or $P4_32_12$.

Molecular replacement was carried out with various known models of CARD domains in the PDB, for both space groups, using the program PHASER [19]. A solution was obtained with the ICEBERG CARD (PDB-ID **1DGN**) in the space group $P4_12_12$. There is one CARD molecule in the asymmetric unit. Model building was carried out using the program Coot [20] and refinement was carried out using the program REFMAC5 from the CCP4 package [21]. In the refined map, two residues that link the C-terminal poly-histidine tag to the protein were also observed. The quality of the structure was assessed using the programs PROCHECK [22] and WHATIF [23]. All indicators suggest that the quality of the structure is good. The details of the crystallographic data collection and refinement are presented in Table 1. The structure has been deposited in the Protein Data Bank and the accession code is **2NSN**.

Results and discussion

The overall structure of the Nod1 CARD was expected to be similar to the other CARD structures, as well as to the recently published NMR structure of the Nod1 CARD [13].

However, as we started building the electron density it became apparent that, while the first five helices were similar, the sixth helix was different. The sixth helix in our structure is an extension of the fifth helix, with a kink. In order to confirm this, we calculated several difference electron density maps. Figure 1(a) shows the (2Fo-Fc) electron density map, at one sigma level, in the region where the loop exists in other CARD structures. There is no obvious break in the density and the helix was the only possible way to trace the chain in the electron density map. This cannot be attributed to model bias from molecular replacement, as this is different from the starting model. Figure 1(b) shows a cartoon representation of the molecule in the asymmetric unit. Interestingly, the helical kink observed in the NMR structure is also observed in the crystal structure, at position 100. This suggests that the kink in the sixth helix is independent of the two possible orientations for this helix.

When the neighboring molecules related by crystal packing were generated, it was immediately noticed that the sixth helix from another molecule occupies the approximate position of the sixth helix seen in all other CARD structures (Figure 2(a) and 2(b)). Therefore, the molecule observed in the crystal structure is a dimer. The dimer is formed by a swapping of the sixth helices between two molecules. Dynamic light scattering experiments of the purified protein also suggested a dimer (data not shown). There are a number of interactions between helix six of one molecule and residues of the other. The sixth helix of one molecule interacts with helices one and five as well as with residues from the loop region connecting helices one and two. As one would expect, the interactions are symmetrical between the two dimers. They consist of van der Waals, hydrogen bonding and ionic interactions. Both the main-chain and side-chain atoms of N36 (present in the C-terminal end of helix one) interact with residues Q92 and Y97. Arginine 35 makes hydrogen bonds with the main-chain and side-chain of D95 along with the side-chain of D99. The main-chain nitrogen of A96 and the main-chain carbonyl oxygen of R35 are involved in a hydrogen bond. There are also a number of hydrophobic interactions that stabilize this interface. Leucine 29 and 30 are involved in hydrophobic interactions with L100 and W103 of the other molecule. Interestingly, interactions found in the monomeric NMR structure of Nod1 CARD, between W103, F109, and residues around L22 in helix one [13], are preserved in the dimeric structure that we report here. The total buried surface area, calculated using surfvol [24], is about 3000 $Å^2$ for the dimer, with approximately 1500 $Å^2$ of each monomer being buried.

The overall Greek key fold of the CARD domain is conserved in the dimeric structure of the Nod1 CARD. The hydrophobic core that stabilizes interactions between helices in other CARD structures is also conserved in this structure. An acidic patch, formed by residues E53, D54, and E56 (located on helices two and three (Figure 1(b))), has been shown to be important for the interaction between Nod1 CARD and the CARD of RICK kinase [13]. This acidic patch is conserved in APAF-1 CARD and was shown to be important for its interaction with procaspase-9 CARD [15].

We superposed the first five helices of the Nod1 CARD crystal structure with the CARD structures of APAF1 [15], procaspase-9 [15], RAIDD [11] and ICEBERG [12]. The best discrimination in our molecular replacement calculations was obtained using the model of ICEBERG (inhibitor of interleukin-1 beta generation). The RMS deviation of the five helices (74 C-alpha atoms) to ICEBERG was 1.3 Å. The RMS deviation of the five helices to APAF1 card was 1.5 Å (for 78 C-alpha atoms), to procaspase-9 was 1.5 Å (71 C-alpha atoms) and to RAIDD was 2.0 Å (68 C-alpha atoms). Figure 3 shows a superposition of these structures. While there are small differences in the orientation of the different helices, the overall structures are very similar, if one were to consider only the first five helices. Our superposition calculations suggest that the Nod1 CARD crystal structure agrees much better with other CARD structures, compared to the Nod1 CARD NMR structure. However, as seen in Figure

3, the sixth helix of the crystal structure points away compared with the sixth helices of the other CARDs.

This is the first report of a homodimeric structure for a CARD. The identification of both monomeric and dimeric forms of the same domain, suggests a possible mechanism for regulating interactions between Nod1 and the proteins it associates with, including: RICK, procaspase-9, and procaspase-1 [4,9]. The structure shows that the region proposed to interact with RICK CARD is exposed in the dimer. Since Nod1 activates RICK after ligand recognition, it is conceivable that this interface is buried while the receptor is inactive. Burial of the interacting CARD face by the NOD domain has been proposed as the mechanism of APAF1 regulation [25]. Given the evidence that the full-length Nod1 receptor co-immunoprecipitates with itself [4], the crystal structure is probably representative of a physiologically relevant form of Nod1 CARD. Ligand recognition would result in a change in oligomerization of the CARD and expose the acidic patch for an interaction with the RICK CARD, leading to RICK activation. We hypothesize that this exposure will result from a combination of conformational rearrangements and change of oligomerization state. Further experimental studies are in progress to test the mechanism of signaling by pro-inflammatory CARDs.

Supplementary Material

Refer to Web version on PubMed Central for supplementary material.

Acknowledgements

We would like to thank Derek Yoder for help with data collection at GM/CA CAT. GM/CA CAT has been funded in whole or in part with Federal funds from the National Cancer Institute (Y1-CO-1020) and the National Institute of General Medical Science (Y1-GM-1104). Use of the Advanced Photon Source was supported by the U.S. Department of Energy, Basic Energy Sciences, Office of Science, under contract No. □W-31-109-ENG-38. Christine McDonald would like to acknowledge support by a Career Development Award from the Crohn's and Colitis Foundation of America. We would also like to thank Jon C. D. Houtman, Kevin P. Battaile, and Ehmke Pohl for their help with our studies. S.R. would like to acknowledge funding from USPHS grant #GM62904.

References

1. Medzhitov R, Janeway CA Jr. Innate immunity: the virtues of a nonclonal system of recognition. Cell 1997;91:295–298. [PubMed: 9363937]
2. Uematsu S, Akira S. Toll-like receptors and innate immunity. J Mol Med. 2006
3. Chamaillard, Inohara; McDonald, C.; Nunez, G. NOD-LRR proteins: role in host-microbial interactions and inflammatory disease. Annu Rev Biochem 2005;74:355–383. [PubMed: 15952891]
4. Inohara N, Koseki T, del Peso L, Hu Y, Yee C, Chen S, Carrio R, Merino J, Liu D, Ni J, Nunez G. Nod1, an Apaf-1-like activator of caspase-9 and nuclear factor-kappaB. J Biol Chem 1999;274:14560–14567. [PubMed: 10329646]
5. Bertin J, Nir WJ, Fischer CM, Tayber OV, Errada PR, Grant JR, Keilty JJ, Gosselin ML, Robison KE, Wong GH, Glucksmann MA, DiStefano PS. Human CARD4 protein is a novel CED-4/Apaf-1 cell death family member that activates NF-kappaB. J Biol Chem 1999;274:12955–12958. [PubMed: 10224040]
6. Girardin SE, Boneca IG, Carneiro LA, Antignac A, Jehanno M, Viala J, Tedin K, Taha MK, Labigne A, Zahringer U, Coyle AJ, DiStefano PS, Bertin J, Sansonetti PJ, Philpott DJ. Nod1 detects a unique muropeptide from gram-negative bacterial peptidoglycan. Science 2003;300:1584–1587. [PubMed: 12791997]
7. Chamaillard M, Hashimoto M, Horie Y, Masumoto J, Qiu S, Saab L, Ogura Y, Kawasaki A, Fukase K, Kusumoto S, Valvano MA, Foster SJ, Mak TW, Nunez G, Inohara N. An essential role for NOD1 in host recognition of bacterial peptidoglycan containing diaminopimelic acid. Nat Immunol 2003;4:702–707. [PubMed: 12796777]

8. Girardin SE, Tournebize R, Mavris M, Page AL, Li X, Stark GR, Bertin J, DiStefano PS, Yaniv M, Sansonetti PJ, Philpott DJ. CARD4/Nod1 mediates NF-kappaB and JNK activation by invasive Shigella flexneri. EMBO Rep 2001;2:736–742. [PubMed: 11463746]
9. Yoo NJ, Park WS, Kim SY, Reed JC, Son SG, Lee JY, Lee SH. Nod1, a CARD protein, enhances pro-interleukin-1beta processing through the interaction with pro-caspase-1. Biochem Biophys Res Commun 2002;299:652–658. [PubMed: 12459189]
10. Weber CH, Vincenz C. The death domain superfamily: a tale of two interfaces? Trends Biochem Sci 2001;26:475–481. [PubMed: 11504623]
11. Chou JJ, Matsuo H, Duan H, Wagner G. Solution structure of the RAIDD CARD and model for CARD/CARD interaction in caspase-2 and caspase-9 recruitment. Cell 1998;94:171–180. [PubMed: 9695946]
12. Humke EW, Shriver SK, Starovasnik MA, Fairbrother WJ, Dixit VM. ICEBERG: a novel inhibitor of interleukin-1beta generation. Cell 2000;103:99–111. [PubMed: 11051551]
13. Manon F, Favier A, Nunez G, Simorre JP, Cusack S. Solution Structure of NOD1 CARD and Mutational Analysis of its Interaction with the CARD of Downstream Kinase RICK. J Mol Biol. 2006
14. Vaughn DE, Rodriguez J, Lazebnik Y, Joshua-Tor L. Crystal structure of Apaf-1 caspase recruitment domain: an alpha-helical Greek key fold for apoptotic signaling. J Mol Biol 1999;293:439–447. [PubMed: 10543941]
15. Qin H, Srinivasula SM, Wu G, Fernandes-Alnemri T, Alnemri ES, Shi Y. Structural basis of procaspase-9 recruitment by the apoptotic protease-activating factor 1. Nature 1999;399:549–557. [PubMed: 10376594]
16. Day CL, Dupont C, Lackmann M, Vaux DL, Hinds MG. Solution structure and mutagenesis of the caspase recruitment domain (CARD) from Apaf-1. Cell Death Differ 1999;6:1125–1132. [PubMed: 10578182]
17. Zhou P, Chou J, Olea RS, Yuan J, Wagner G. Solution structure of Apaf-1 CARD and its interaction with caspase-9 CARD: a structural basis for specific adaptor/caspase interaction. Proc Natl Acad Sci U S A 1999;96:11265–11270. [PubMed: 10500165]
18. Pflugrath JW. The finer things in X-ray diffraction data collection. Acta Crystallogr D Biol Crystallogr 1999;55:1718–1725. [PubMed: 10531521]
19. Read RJ. Pushing the boundaries of molecular replacement with maximum likelihood. Acta Crystallographica Section D-Biological Crystallography 2001;57:1373–1382.
20. Emsley P, Cowtan K. Coot: model-building tools for molecular graphics. Acta Crystallographica Section D-Biological Crystallography 2004;60:2126–2132.
21. Murshudov GN, Vagin AA, Dodson EJ. Refinement of macromolecular structures by the maximum-likelihood method. Acta Crystallographica Section D-Biological Crystallography 1997;53:240–255.
22. Laskowski RA, Macarthur MW, Moss DS, Thornton JM. Procheck - a Program to Check the Stereochemical Quality of Protein Structures. Journal of Applied Crystallography 1993;26:283–291.
23. Vriend G. What If - a Molecular Modeling and Drug Design Program. Journal of Molecular Graphics 1990;8:52. [PubMed: 2268628]&
24. Gerstein M. A Resolution-Sensitive Procedure for Comparing Protein Surfaces and Its Application to the Comparison of Antigen-Combining Sites. Acta Crystallographica Section A 1992;48:271–276.
25. Riedl SJ, Li W, Chao Y, Schwarzenbacher R, Shi Y. Structure of the apoptotic protease-activating factor 1 bound to ADP. Nature 2005;434:926–933. [PubMed: 15829969]
26. Brunger AT. Free R-Value - a Novel Statistical Quantity for Assessing the Accuracy of Crystal-Structures. Nature 1992;355:472–475.
27. Merritt EA, Murphy MEP. Raster3d Version-2.0 - a Program for Photorealistic Molecular Graphics. Acta Crystallographica Section D-Biological Crystallography 1994;50:869–873.
28. DeLano, WL. The PyMol Molecular Graphic System. DeLano Scientific; San Carlos, CA, USA: 2002.

Figure 1.
(a) The (2Fo-Fc) electron density map, at one sigma level, in the region beyond helix 5, where a loop is present in the other CARD structures. This map shows the continuous density from helix 5 to helix 6, which interacts with a second molecule. (b) A cartoon representation of the Nod1 CARD structure in the asymmetric unit. The structure is colored as a rainbow from blue (N-terminus) to red (C-terminus). Residues L40, L44, D48, E53, D54, and E56 from helices 2 and 3 are shown in ball and stick. These residues either form the acidic patch or have been shown to play a role in the interaction between Nod1 CARD and RICK CARD [13]. Figure 1 (a) was made using a combination of Coot [20] and RASTER3D [27]. All other figures were made using the program PYMOL [28].

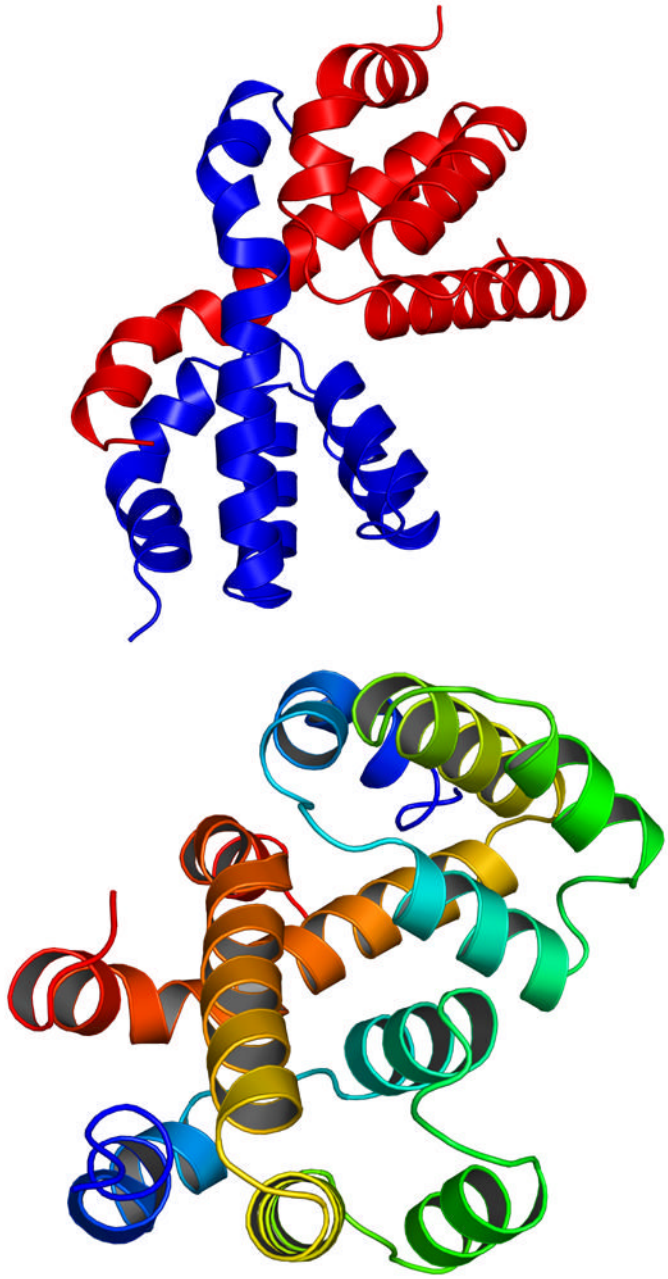

Figure 2.
(a) A cartoon representation of the dimeric form of the Nod1 CARD structure, showing the helix swapping. The two molecules of the dimer are shown in different colors. It is clear from the figure that helix 6 of the blue molecule interacts with helices 1 and 5 of the red molecule and vice versa. (b) A view perpendicular to that shown in (a).

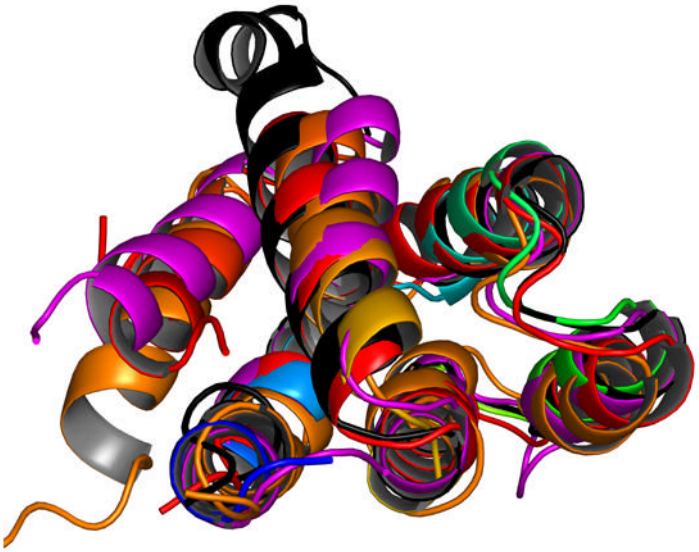

Figure 3.
A cartoon representation showing the superposition of different CARD structures that are present in the PDB and discussed in this paper. The molecule shown in black is Nod1 CARD. Helix six is the most flexible helix in the structures; and in the superposition, it points in a completely different direction compared to the other four structures shown.

Table 1

Data collection and refinement statistics

(A) Data collection statistics	
Resolution (Å)	28 – 2.0
Wavelength (Å)	0.979
Space Group	$P4_12_12$
Cell (Å)	a = b = 40.4; c = 150.7
Completeness (%) (last shell)	98.2 (2.07–2.0:99.5)
Redundancy	13.38 (13.1)
I/σ_I	21.3 (4.8)
R_{merge} (%)[b]	5.9 (35.5)
(B) Refinement statistics	
Resolution range (Å)	11–2.0
R (%)[c]	22.05
R_{free} (%)[d]	26.2
rms bonds (Å)	0.012
rms angles (°)	1.34
Number of water molecules	37
Number of protein atoms	1563
Ramachandran analysis (%)	
Most favored	95.4
Allowed	4.6

[a] Values in parentheses relate to the highest resolution shell.

[b] $R_{merge} = \sum|I| - \langle I\rangle/\sum I$, where I is the observed intensity, and $\langle I\rangle$ is the average intensity obtained from multiple observations of symmetry-related reflections after rejections.

[c] $R = \sum||F_O| - |F_C||/\sum|F_O|$, where F_O and F_C are the observed and calculated structure factors, respectively.

[d] R_{free} defined in Brunger [26].